# A Double Seismic Array Experiment on Mt. Etna

Osservatorio Vesuviano
Open file report n 2-2000

Participant institutions

Osservatorio Vesuviano

Mario Castellano*,  Marco Capello, Edoardo Del Pezzo**, Flora Giudicepietro, Mario La Rocca, Marcello Martini,  Simona Petrosino, Gilberto Saccorotti.

Instituto Andaluz de Geofisica - Universidad de Granada

Jesus Ibanez, Miguel Abril, Javier Almendros, Enrique Carmona, Carmen Martinez, Jaime Vilchez.

Progetto POSEIDON – INGV

Eugenio Privitera, Salvo Alparone , Giuseppe Di Grazia, Stefano Gresta.

***Field Survey Organiser**

****Responsible of the Project**

CNR-GNV Grant # 2-13-3-46-23  Osservatorio Vesuviano

**Abstract**

On September 1999 two seismic antennas (array) and a profile of 3-D stations equipped with short period seismometers were installed on Mt. Etna; Aims of the experiment were to investigate the structure and the polarisation parameters of the volcanic tremor wavefield radiated in eruptive conditions, and to measure the seismic velocities and attenuation in the shallow structure beneath the arrays. The first array was installed close to Pizzi Deneri Volcanological Observatory, East of the crater area; the second array was located close to Torre del Filosofo site, south of the crater area. The profile was set up close to the Pizzi Deneri array. It had a length of 600 meters and consisted of 16 short period 3-component stations. In addition, a circular array of 8 short period seismometers was set up around the main crater area (Fig. 1). Several tremor samples and explosions quakes were recorded in 10 days of operation .

Spectrograms show predominant energy into 1-4 Hz frequency band. Slowness spectra indicate a predominant source of the tremor located at surface and coincident with the crater area. Polarisation analysis show that the direction of predominant motion is transverse with respect to the direction pointing to the active craters.

**Introduction**

Seismic arrays have been widely used to study the wavefield associated to volcanic tremor and explosion quakes (*Goldstein & Chouet*, 1994; *Ferrazzini et. al., 1991*; *Chouet et al.,1997*; *Del Pezzo et. al, 1997*). They are essential tools to track the seismic source of the volcanic signals as Long Period events and volcanic tremor. As the insurgence of this kind of events is very often related to the occurrence of volcanic eruptions, the real-time multichannel analysis applied to array data assumes increasing importance in volcano monitoring.

The knowledge of the wavefield structure of the tremor is the first goal to achieve together with the knowledge of the elastic properties of the shallow layers through which seismic waves propagate. For this reason, a series of experiments was conducted over the last 6 years in the framework of an international co-operation and with the main financial support of Italian GNV and Spanish Antarctic Project. These experiments were aimed at a testing of array techniques and on investigating the properties of volcanic signals (tremor and explosion quakes) on several volcanoes like *Stromboli (O.V. Open File Report n. 1-98*), Vesuvius (*O.V.*

*Open File Report n. 1-99*), Deception Island (*O.V. Open File Report n. 3-99 and n. 1 2000*), Teide (*Almendros et al., 2000*) and the present one at Mt. Etna.

The present report provides information about the array set up and operation, instrument calibration and data format.

**Site selection**

A preliminary survey was carried out on the end of May, 1999, in order to select the sites for the installation of the two seismic antennas and the profile. We searched two flat and geologically homogeneous zones, about 300 meters wide, positioned at about 90° apart with respect to the position of the source, which was assumed to be located in close proximity of the crater area (fig.1). Using this geometry, the estimate of the spatial location of the source is optimised, as shown in *O.V open file report n. 1-98 and in Saccorotti et al.,1998*. The area around Pizzi Deneri Volcanological Observatory (area1) and the area around Torre del Filosofo site (area 2) resulted the most suitable for the installation. Area 1 was selected also for the deployment of the seismic profile, due to the easier accessibility.

**Instrument positioning and installation. Array configuration.**

1. Time schedule of the instrument installation
   September 8. Installation of array P (fig. 2) at Pizzi dei Neri site
   September 9 – September 10 . Installation of array abc+L (fig. 3) at Pizzi Deneri site
   September 10 – September 11. Installation of array def (fig. 4)at Torre del Filosofo
   September 16 – September 17. Installation of array abc+U(fig. 5) at Pizzi Deneri
   September 17 – “Circular” (fig. 6) array around craters.
2. Co-ordinates of all the array stations except the array “Circular” were measured using a total EDM station and referred to an absolute GPS benchmark located nearby. Array “Circular” co-ordinates were obtained directly by GPS positioning. Uncertainties are less than 5 cm for the co-ordinates measured with the total station, and about 100 meters for the circular array station co-ordinates. In Table 1 is reported the list of the co-ordinates of all the array configurations.

**Data collection and storage.**

Array abc and def are composed by MARK L-4 C sensors cable-connected to 8 channel data loggers. The instruments were designed by Ramon Ortiz and G. Alguacil, and described in *Del Pezzo et al. (1997)* where the original references (in spanish) can be found. Details about the electronic scheme are reported in *Ortiz et al. (1997*). Seismic signals are amplified, sampled with a 16 bits A/D converter and anti-alias filtered before the storage onto the hard disk of a portable P.C. Time synchronisation is performed by a GPS antenna connected to the data logger.

Array P,U and "Circular" are equipped with 3-channel, MARS LITE data loggers, and 3-D, 4.5 electronically extended to 1 Hz sensors.

The time operation of the instruments is reported in Fig. 7 and 8.

**Transfer function of the instruments.**

Calibration of Mars Lite seismometers has been checked using a Teledune Geotech 3-D S13 seismometer as reference. A long noise sample has been recorded both at Mars-Lite seismometer and S-13 using identical data loggers. The ratio between the Fourier Transforms of the noise samples at homologue components is the ratio of the transfer functions of the sensors. S-13 (critically damped) has been calibrated through the access to the moving mass (see S-13 operation and maintenance manual) . Results show that S-13 and MARS-Lite seismometers have the same amplitude response at frequencies higher than 1 Hz, as shown in fig. 9 where the amplitude spectral ratio between the two vertical components is plotted as a function of frequency. Phase responses of the two instruments are compared in fig. 10. Velocity transduction results of 400 V/m/s, coincident with that reported in the Mars-Lite data sheet.

Mark L4 seismometers were damped at 65% critical damping (arrays abc and def). Amplitude and phase response curves are reported in fig. 11.

**Description of the Etna eruptive activity during the experiment.**

Etna volcano was active during the experiment . This eruptive phase started on January 1999 with a moderate activity at Bocca Nuova. Seven eruptive episodes (January 5 – February 4) occurred at S-E crater and terminated with the opening of a fracture at the cone base, directed toward S-E. Strombolian activity together with lava fountains accompanied a lava flow started on February 4, which rapidly reached Valle del Bove. The lava flow continued for the whole period of the experiment. On September 4 new activity started at Voragine crater, characterised by important lava fountains (information and maps on line at http://193.204.162.114/gnv/index-etna.html)

**Purposes and Methods.**

The experiment was aimed at a) the investigation of the kinematic properties of the volcanic tremor wavefield from frequency-slowness analysis; b) the constrain of the location of its source, c) the measurement of the seismic attenuation and d) the study of the polarisation properties of the tremor wavefield.

Slowness spectra can be calculated using time or frequency domain techniques. In time domain we use the so called Zero-Lag Cross-correlation technique (*Del Pezzo et al., 1997*); in frequency domain we use MUSIC algorithm (*Goldstein and Archuleta, 1987*) .

The double array configuration will allow the space tracking of the source using the probabilistic method described in *Saccorotti et al., 1998*.

The Profile oriented toward the craters (L-array of fig. 3) will permit the estimate of the spatial attenuation of tremor energy, and hence the seismic quality factor of the earth medium.

Circular array will allow the study of the particle motion pattern of the tremor waves around the craters. Polarisation parameters of the waves composing the tremor wavefield will be fully investigated using the 3-D stations (*La Rocca, 2000*).

Application of the correlation method of *Aki (1957, 1965)* to both Pizzideneri and Torre Del Filosofo arrays will allow to derive the dispersive properties of Rayleigh and Love waves, from which a shallow velocity structure beneath the arrays may eventually be obtained.

**Preliminary results**

An example of data recorded at L005 station is shown in fig. 12.

The spectrogram of a sample of tremor recorded at array A shows the highest energy concentrated between 1 and 4 Hz, with some additional bursts between 4 and 6 Hz (fig. 13) .

Preliminary frequency-slowness analysis carried out on a tremor sample recorded at array p, shows a predominant back-azimuth in the direction of the crater area (fig.14).

Polarisation analysis shows a predominant particle motion direction around 110 degrees, approximately normal to the back-azimuth. The incidence is around 90 degrees, showing an almost horizontal wave motion. Taken together with the high values of the rectilinearity coefficient, these observations are suggestive of a wavefield dominated by SH-Love (fig.15).

The correlation coefficients averaged over the array stations as a function of the frequency have been calculated for array abc for receiver spacing of 50, 100, and 150 m (Fig.

16). The smooth thin lines superimposed to the data represent the theoretical correlation coefficients derived from eq. 4 of *Chouet et al., (1998*), using the dispersion curve shown in the last panel of the same figure. The procedure is described in *Chouet et al., 1998*. From this dispersion curve the velocity model can be inferred with an inversion procedure.

**Future developments**

We have planned to extend the above approaches to the whole data set in order to characterise the wavefield structure of the volcanic tremor at Etna volcano. Moreover we will extend the same methods to the explosion quakes which in many cases were superimposed to the background tremor radiation. The aim of this second analysis is twofold: first we could constrain the space position of the source of the explosion quake; second, we could compare the spectral characteristics of the volcanic tremor with those of the explosion quakes, in order to contribute to the understanding of the explosion quake source processes. *Ferrucci et al. (1990),* analyse the polarisation properties of the tremor at Etna, using a 3 stations array located onto the south-western flanks of the volcano. They tentatively link the tremor source to the main dyke-system of Etna and exclude the confinement of the tremor source to the only active vent. A check of this result may be obtained by the analysis of the present data, and particularly from the array "circular", which would better enlighten the polarisation pattern of the tremor around the crater area.

**Acknowledgements**

Orazio Consoli is gratefully acknowledged for his help at Pizzi Deneri Observatory. Ente Parco dell'Etna is acknowledged for its NULLA OSTA for the experiment.

## References

Almendros, J., Ibanez, J.M., Alguacil, G., Morales, J., Del Pezzo, E., La Rocca, M., Ortiz, R., Arana, V., Blanco, M.J.,2000. A double seismic antenna experiment at Teide Volcano: existence of local seismicity and evidence for the non existence of volcanic tremor. In press for J. Volcanol and Geoth. Res.

Aki, K., 1957. Space and time spectra of stationary stochastic waves, with special reference to microtremors, Bull. Earthquake Res. Inst. Tokyo Univ. 25, 415-457

Aki, K., 1959 Correlational study of near earthquake waves Bull. Earthquake Res. Inst. Tokyo Univ, 37, 207-232

Chouet B.A., Saccorotti G., Martini M., Dawson P.B., De Luca G., Milana G. and Scarpa R., 1997. Source and path effects in the wavefields of tremor and explosions at Stromboli volcano, Italy. J. Geophys. Res., 102, 15129-15150

Chouet, B.A., De Luca, G., Dawson, P.B., Milana, G., Martini, M. and Scarpa R., 1998. Shallow velocity structure of Stromboli volcano, Italy, derived from small-aperture array measurements of Strombolian tremor. Bull. Seism. Soc. Amer., 88, 653-666.

Del Pezzo E., La Rocca M., Ibanez J., 1997. Observation of high-frequency scattered waves using dense arrays at Teide volcano. Bull. Seism. Soc. Amer., 87,6,1637-1647.

Ferrazzini, V.,Aki, K., Chouet, B. 1991. Characteristics of seismic waves composing Hawaian volcanic tremor and gas-piston events observed by a near source array, J. Geophys. Res.,96, 6199-6209

Ferrucci, F.,Godano, C., Pino, N.A. Approach to the volcanic tremor by covariance analysis:application to the 1989 eruption of Mt. Etna (Sicily), 1990. Geophys. res. Letters, 17,12, 2425-2428.

Goldstein, P., and Archuleta, R.J., 1987. Array analysis of seismic signals. Geophys. Res. Lett., 14, 13-16.

Goldstein P., Chouet B., 1994. Array measurements and modeling of a source of shallow volcanic tremor at Kilauea Volcano, Hawaii. J. Geophys. Res. , 99:2637-2652

La Rocca, M. 2000. Multichannel array techniques applied to volcanic hazard. Ph.D. Thesis. University of Salerno. Science faculty.

La Rocca M., Petrosino S., Saccorotti G., Simini M., Ibanez J., Almendros J. and Del Pezzo E., 1998. Location of the source and shallow velocity model deduced from the explosion quakes recorded by two seismic antennas at Stromboli volcano. Phys. Chem. of the Earth (Invited paper- in press)

Ortiz, R., Garcia, A., Astiz, M., 1997 Estacion de registro sismico continuo. Instrumentacion en volcanologia vol II. Ortiz (edt) Report Projecto Teide, Volcan lab europeo. CSIC, Madrid, pp.103-107

O.V. Open File Reports: all availble on line at http://www.osve.unina.it

Saccorotti, G., Chouet, B.A., Martini, M. and Scarpa R., 1998. Bayesian Statistics applied to the location of the source of explosions at Stromboli volcano, Italy. Bull. Seism. Soc. Amer.,5,1099-1111.

**Figure Captions**

Fig. 1 . Sketch map of the Etna area around craters. In the zones of Torre del Filosofo and Pizzi Deneri the array configurations are plotted together. In particular at Pizzi Deneri we overplot 3 different configurations, used separately in different time periods. Note that the array represented by black triangles, (see details in the next Fig. 6) , is in reality composed by 8 stations: the northernmost and southernmost stations are not represented by black triangles as their symbol would have covered part of the semicircular array configurations.

Fig. 2 . Sketch map of array P at Pizzi Deneri site. Mars Lite stations were used in this configuration.

Fig. 3 . Array abc and L (profile) at Pizzi Deneri site. L array was made by Mars Lite. abc is composed by 3 8-channels data loggers, connected to MARK L4 sensors (see text).

Fig. 4 . Array def, at Torre del Filosofo site. Configuration is similar to and instruments are the same of array abc.

Fig. 5 . Array abc and U. Mars lite stations were deployed in a tripartite profile configuration. This configuration was called MEDUSA.

Fig. 6 . Array “circular”. This configuration was obtained using Mars-Lite stations.

Fig. 7 . Time table of the overall operation for array abc and def

Fig. 8 . Time table for the overall operation of a) array P, b) array L, c) array R and d) array U.

Fig. 9 . Spectral ratio between long duration noise samples recorded at the same site, using the same data logger connected to a S13 couple (1 vertical and 1 horizontal) and to a 3-D Mars-lite seismometer.

Fig. 10 . Phase response of Mars lite and vertical S13, reported for comparison.

Fig. 11 Phase and amplitude response for the overall instrument chain used for abc and def arrays.

Fig. 12 . Example of 4-hours continuous data recording. Filtering between 0.1 and 10 Hz is applied in order to reduce the high frequency noise. Vertical lines are the minute marks.

Fig. 13 . Spectrogram of a tremor sample. The spectral power is normalised to the maximum. The grey scale evidences along the sample a maximum power between 1.5 and 4.5 Hz.

Fig. 14 Slowness spectrum obtained using MUSIC method applied to a tremor sample recorded at array abc. Power is reproduced by the grey scale. Maximum power is compatible with the direction of craters.

Fig. 15 . Polarisation parameters as a function of lapse time along the same tremor sample of figure 13. First panel from the top shows the particle motion dominant direction. The second represents the dominant incidence angle. The third reports Rectilinearity and the largest eigenvalue of the co-variance matrix. All quantities are plotted as a function of the lapse time along the sample.

Fig 16 . Correlation coefficient averaged over azimuth for different station spacing. This data permitted to estimate the dispersion curve, shown in the panel below, from which a velocity model can be obtained using an inversion scheme.

Table 1

| Station | lat. deg. | lat. min. | lat. sec. | lon. deg. | lon. min. | lon. sec | Cartesian Y axis (km) | Cartesian X axis(km) |
|---|---|---|---|---|---|---|---|---|
| u05 | 37 | 45 | 53,8193 | 15 | 0 | 54,6124 | 4180,58 | 1336,53 |
| u04 | 37 | 45 | 54,8492 | 15 | 0 | 53,0056 | 4180,61 | 1336,49 |
| u03 | 37 | 45 | 55,8518 | 15 | 0 | 51,4092 | 4180,64 | 1336,45 |
| u02 | 37 | 45 | 56,868 | 15 | 0 | 49,8093 | 4180,67 | 1336,41 |
| u01 | 37 | 45 | 58,049 | 15 | 0 | 47,9244 | 4180,71 | 1336,36 |
| u010 | 37 | 45 | 59,6008 | 15 | 0 | 54,5815 | 4180,76 | 1336,53 |
| u09 | 37 | 45 | 59,4498 | 15 | 0 | 52,9472 | 4180,75 | 1336,49 |
| u08 | 37 | 45 | 59,0378 | 15 | 0 | 51,2238 | 4180,74 | 1336,45 |
| u07 | 37 | 45 | 59,1614 | 15 | 0 | 49,6994 | 4180,74 | 1336,41 |
| u06 | 37 | 45 | 59,0241 | 15 | 0 | 48,2369 | 4180,74 | 1336,37 |
| za | 37 | 45 | 58,873 | 15 | 0 | 46,6129 | 4180,74 | 1336,33 |
| 4a | 37 | 45 | 59,1751 | 15 | 0 | 44,6045 | 4180,74 | 1336,28 |
| zb | 37 | 46 | 0,39734 | 15 | 0 | 45,9332 | 4180,78 | 1336,32 |
| 4c | 37 | 45 | 57,28 | 15 | 0 | 46,2387 | 4180,69 | 1336,32 |
| 5c | 37 | 45 | 55,7007 | 15 | 0 | 45,8714 | 4180,64 | 1336,31 |
| 6c | 37 | 45 | 54,0939 | 15 | 0 | 45,4937 | 4180,59 | 1336,3 |
| zc | 37 | 45 | 57,7606 | 15 | 0 | 45,1263 | 4180,7 | 1336,3 |
| 7c | 37 | 45 | 56,6345 | 15 | 0 | 43,6466 | 4180,67 | 1336,26 |
| 8c | 37 | 45 | 55,5222 | 15 | 0 | 42,1635 | 4180,63 | 1336,22 |
| 5a | 37 | 45 | 58,461 | 15 | 0 | 42,5686 | 4180,72 | 1336,23 |
| 6a | 37 | 45 | 58,2413 | 15 | 0 | 40,5396 | 4180,72 | 1336,18 |
| 7a | 37 | 46 | 0,4248 | 15 | 0 | 43,0115 | 4180,78 | 1336,24 |
| 8a | 37 | 46 | 1,20758 | 15 | 0 | 41,2296 | 4180,81 | 1336,2 |
| 7b | 37 | 46 | 1,92169 | 15 | 0 | 45,2499 | 4180,83 | 1336,3 |
| 8b | 37 | 46 | 3,47351 | 15 | 0 | 44,5599 | 4180,88 | 1336,28 |
| 4b | 37 | 46 | 0,47974 | 15 | 0 | 46,9906 | 4180,78 | 1336,34 |
| 5b | 37 | 46 | 2,07275 | 15 | 0 | 47,3579 | 4180,83 | 1336,35 |
| 6b | 37 | 46 | 3,6795 | 15 | 0 | 47,7322 | 4180,88 | 1336,36 |
| L001 | 37 | 46 | 3,95416 | 15 | 0 | 51,6975 | 4180,89 | 1336,46 |
| L002 | 37 | 46 | 2,93793 | 15 | 0 | 50,6847 | 4180,86 | 1336,43 |
| L003 | 37 | 46 | 1,92169 | 15 | 0 | 49,6616 | 4180,83 | 1336,41 |
| L004 | 37 | 46 | 0,90546 | 15 | 0 | 48,6488 | 4180,8 | 1336,38 |
| L005 | 37 | 45 | 59,903 | 15 | 0 | 47,6292 | 4180,77 | 1336,36 |
| L006 | 37 | 45 | 58,873 | 15 | 0 | 46,6129 | 4180,74 | 1336,33 |
| L007 | 37 | 45 | 57,8568 | 15 | 0 | 45,6001 | 4180,7 | 1336,31 |
| L008 | 37 | 45 | 56,8543 | 15 | 0 | 44,5805 | 4180,67 | 1336,28 |
| L009 | 37 | 45 | 55,8243 | 15 | 0 | 43,5642 | 4180,64 | 1336,26 |
| L010 | 37 | 45 | 54,8218 | 15 | 0 | 42,5446 | 4180,61 | 1336,23 |
| L011 | 37 | 45 | 53,8055 | 15 | 0 | 41,5318 | 4180,58 | 1336,21 |
| L012 | 37 | 45 | 52,7756 | 15 | 0 | 40,5087 | 4180,55 | 1336,18 |
| L013 | 37 | 45 | 51,7731 | 15 | 0 | 39,4959 | 4180,52 | 1336,16 |
| L014 | 37 | 45 | 50,7568 | 15 | 0 | 38,4762 | 4180,49 | 1336,13 |
| L015 | 37 | 45 | 49,7406 | 15 | 0 | 37,46 | 4180,45 | 1336,11 |
| L016 | 37 | 45 | 48,7244 | 15 | 0 | 36,4403 | 4180,42 | 1336,08 |
| zd | 37 | 43 | 57,6526 | 15 | 0 | 29,7455 | 4177,01 | 1335,92 |
| 6f | 37 | 43 | 59,8224 | 15 | 0 | 24,4103 | 4177,07 | 1335,78 |
| 5f | 37 | 43 | 59,0945 | 15 | 0 | 26,1887 | 4177,05 | 1335,83 |
| 4f | 37 | 43 | 58,3804 | 15 | 0 | 27,9568 | 4177,03 | 1335,87 |

| | | | | | | | | |
|---|---|---|---|---|---|---|---|---|
| 2f | 37 | 43 | 59,3417 | 15 | 0 | 27,6203 | 4177,06 | 1335,86 |
| 3f | 37 | 44 | 0,4541 | 15 | 0 | 26,2127 | 4177,09 | 1335,83 |
| 8f | 37 | 44 | 1,89606 | 15 | 0 | 27,0298 | 4177,14 | 1335,85 |
| 7f | 37 | 44 | 0,4953 | 15 | 0 | 27,919 | 4177,1 | 1335,87 |
| zf | 37 | 43 | 59,0808 | 15 | 0 | 28,8288 | 4177,05 | 1335,89 |
| 2d | 37 | 44 | 1,60767 | 15 | 0 | 28,9593 | 4177,13 | 1335,9 |
| 6d | 37 | 44 | 2,41791 | 15 | 0 | 30,6931 | 4177,15 | 1335,94 |
| 5d | 37 | 44 | 0,82489 | 15 | 0 | 30,3806 | 4177,11 | 1335,93 |
| 4d | 37 | 43 | 59,1083 | 15 | 0 | 30,669 | 4177,05 | 1335,94 |
| 7d | 37 | 43 | 59,9597 | 15 | 0 | 32,6363 | 4177,08 | 1335,99 |
| 8d | 37 | 44 | 1,08582 | 15 | 0 | 34,0679 | 4177,11 | 1336,02 |
| 3d | 37 | 43 | 59,4928 | 15 | 0 | 34,2773 | 4177,06 | 1336,03 |
| 8ee | 37 | 43 | 57,9135 | 15 | 0 | 35,8704 | 4177,02 | 1336,07 |
| 7ee | 37 | 43 | 57,8311 | 15 | 0 | 33,8173 | 4177,01 | 1336,02 |
| ze | 37 | 43 | 57,7487 | 15 | 0 | 31,7608 | 4177,01 | 1335,97 |
| 4ee | 37 | 43 | 56,9247 | 15 | 0 | 31,572 | 4176,99 | 1335,96 |
| 5ee | 37 | 43 | 56,2106 | 15 | 0 | 33,3435 | 4176,96 | 1336 |
| 6ee | 37 | 43 | 55,4553 | 15 | 0 | 35,1872 | 4176,94 | 1336,05 |
| 3ee | 37 | 43 | 57,0346 | 15 | 0 | 34,7443 | 4176,99 | 1336,04 |
| p101 | 37 | 45 | 58,873 | 15 | 0 | 46,6129 | 4180,74 | 1336,33 |
| p102 | 37 | 45 | 57,8293 | 15 | 0 | 45,5692 | 4180,7 | 1336,31 |
| p103 | 37 | 45 | 56,8131 | 15 | 0 | 44,5118 | 4180,67 | 1336,28 |
| p104 | 37 | 45 | 55,7968 | 15 | 0 | 43,4681 | 4180,64 | 1336,25 |
| p107 | 37 | 45 | 57,3898 | 15 | 0 | 42,0399 | 4180,69 | 1336,22 |
| p106 | 37 | 45 | 57,8842 | 15 | 0 | 43,5642 | 4180,7 | 1336,26 |
| p105 | 37 | 45 | 58,3786 | 15 | 0 | 45,0817 | 4180,72 | 1336,29 |
| p108 | 37 | 45 | 58,7769 | 15 | 0 | 44,9856 | 4180,73 | 1336,29 |
| p109 | 37 | 45 | 58,6807 | 15 | 0 | 43,3376 | 4180,73 | 1336,25 |
| p110 | 37 | 45 | 58,6121 | 15 | 0 | 41,6966 | 4180,73 | 1336,21 |
| p113 | 37 | 46 | 0,15015 | 15 | 0 | 41,9128 | 4180,77 | 1336,22 |
| p112 | 37 | 45 | 59,7107 | 15 | 0 | 43,4784 | 4180,76 | 1336,26 |
| p111 | 37 | 45 | 59,2987 | 15 | 0 | 45,0577 | 4180,75 | 1336,29 |
| p114 | 37 | 45 | 59,7794 | 15 | 0 | 45,4216 | 4180,76 | 1336,3 |
| p115 | 37 | 46 | 0,69946 | 15 | 0 | 44,2165 | 4180,79 | 1336,27 |
| p116 | 37 | 46 | 1,60584 | 15 | 0 | 43,0252 | 4180,82 | 1336,24 |
| R00A | 37 | 45,96 | 0 | 15 | 0,84 | 0 | 4180,7 | 1336,43 |
| R001 | 37 | 45,87 | 0 | 15 | 0,035 | 0 | 4180,53 | 1335,23 |
| R002 | 37 | 45,8 | 0 | 14 | 59,365 | 0 | 4180,4 | 1334,24 |
| R003 | 37 | 45,564 | 0 | 14 | 59,14 | 0 | 4179,97 | 1333,9 |
| R004 | 37 | 45,12 | 0 | 14 | 59,13 | 0 | 4179,15 | 1333,89 |
| R005 | 37 | 44,64 | 0 | 14 | 59,18 | 0 | 4178,26 | 1333,96 |
| R006 | 37 | 44,38 | 0 | 14 | 59,75 | 0 | 4177,78 | 1334,81 |
| R007 | 37 | 44,015 | 0 | 15 | 0,43 | 0 | 4177,11 | 1335,82 |
| **CRATER POSITION** | 37 | 45 | 0 | 14 | 59 | 30 | 4178,93 | 1334,44 |

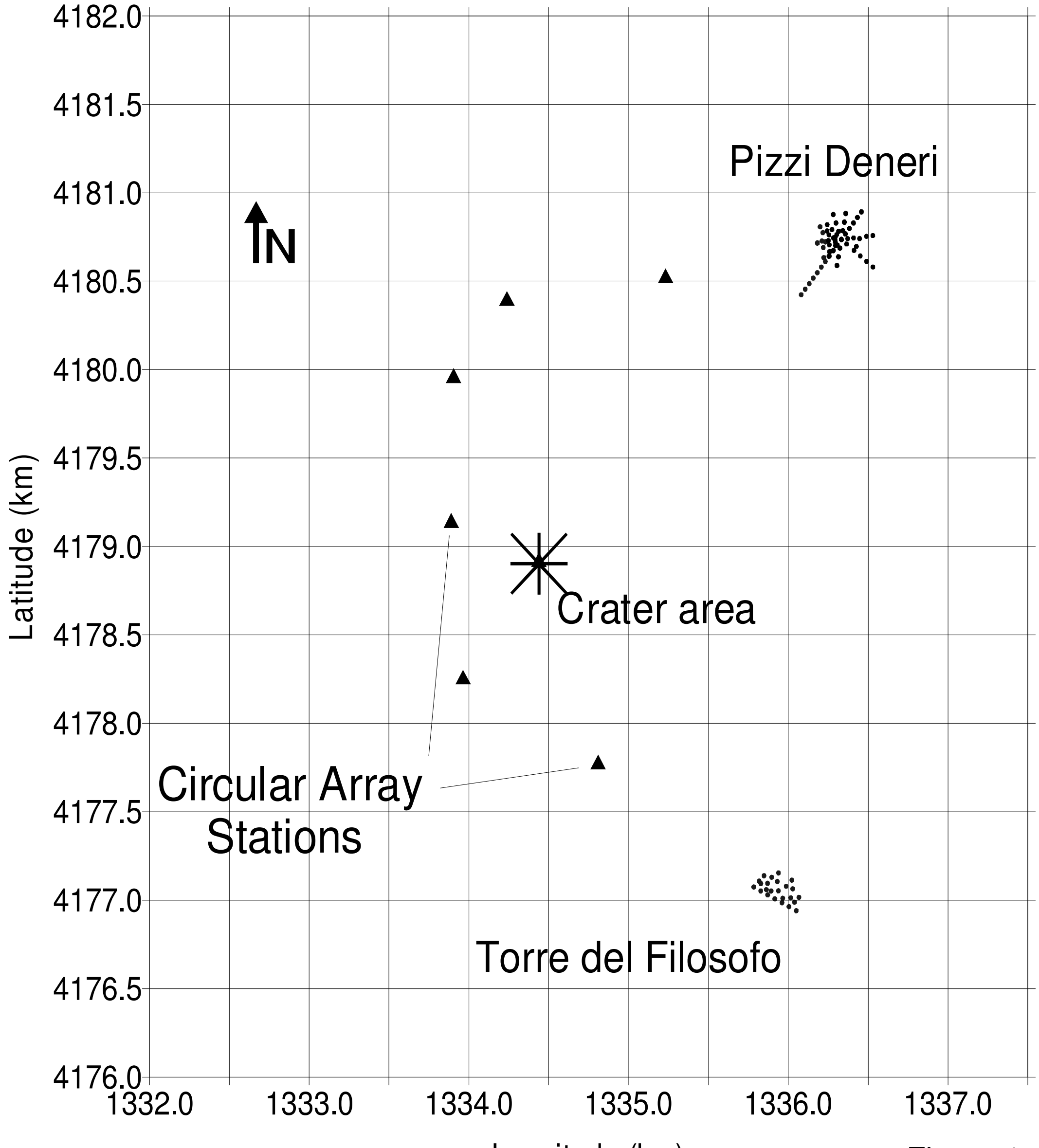
4182.0
4181.5
4181.0
4180.5
4180.0
4179.5
4179.0
4178.5
4178.0
4177.5
4177.0
4176.5
4176.0
Latitude (km)
1332.0
1333.0
1334.0
1335.0
1336.0
1337.0
Longitude (km)
N
Pizzi Deneri
Crater area
Circular Array
Stations
Torre del Filosofo

Figure 1

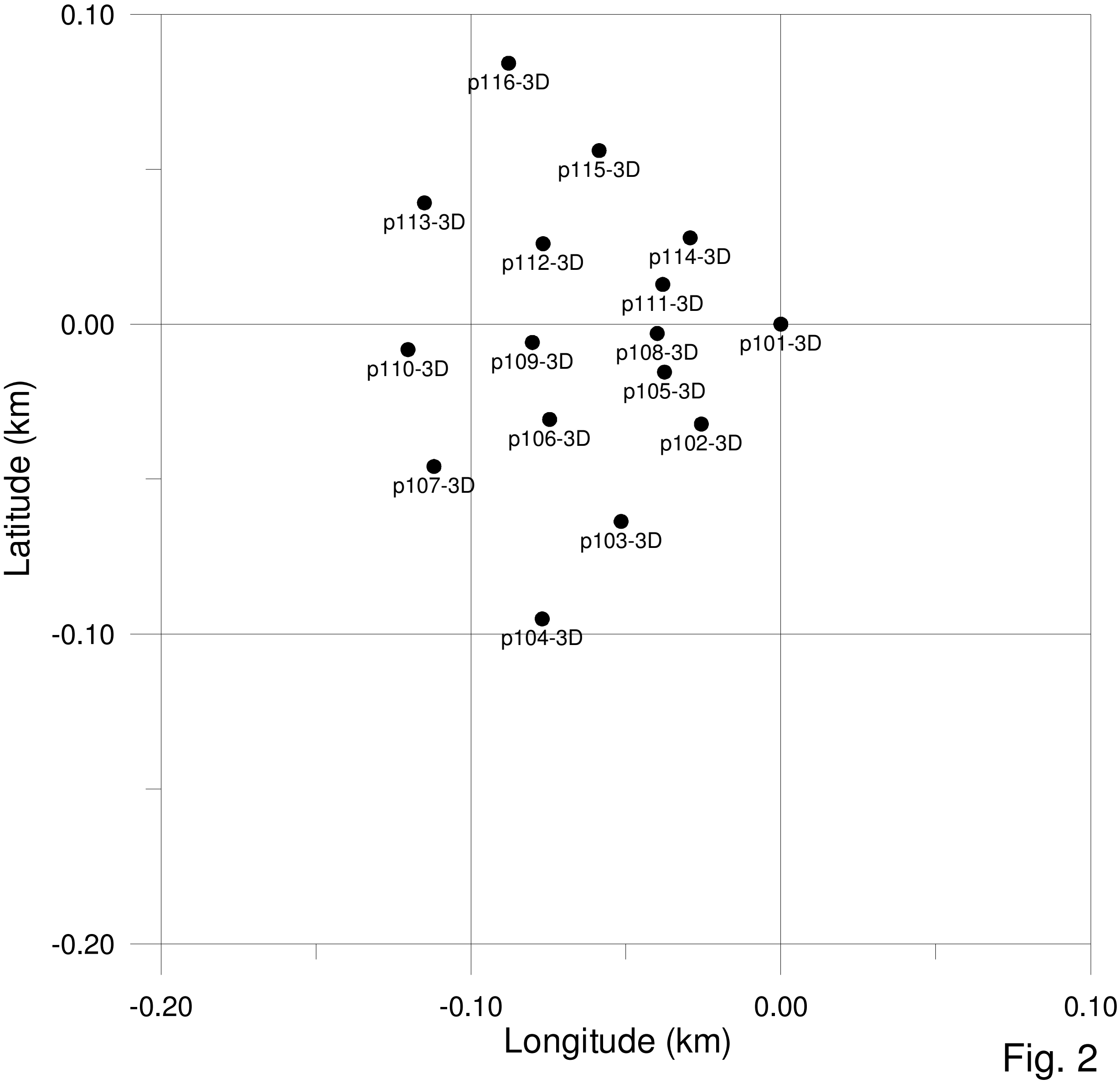

0.10
0.00
-0.10
-0.20
Latitude (km)
p116-3D
p115-3D
p113-3D
p112-3D
p114-3D
p111-3D
p101-3D
p110-3D
p109-3D
p108-3D
p105-3D
p106-3D
p102-3D
p107-3D
p103-3D
p104-3D
-0.20
-0.10
0.00
0.10
Longitude (km)


Fig. 2

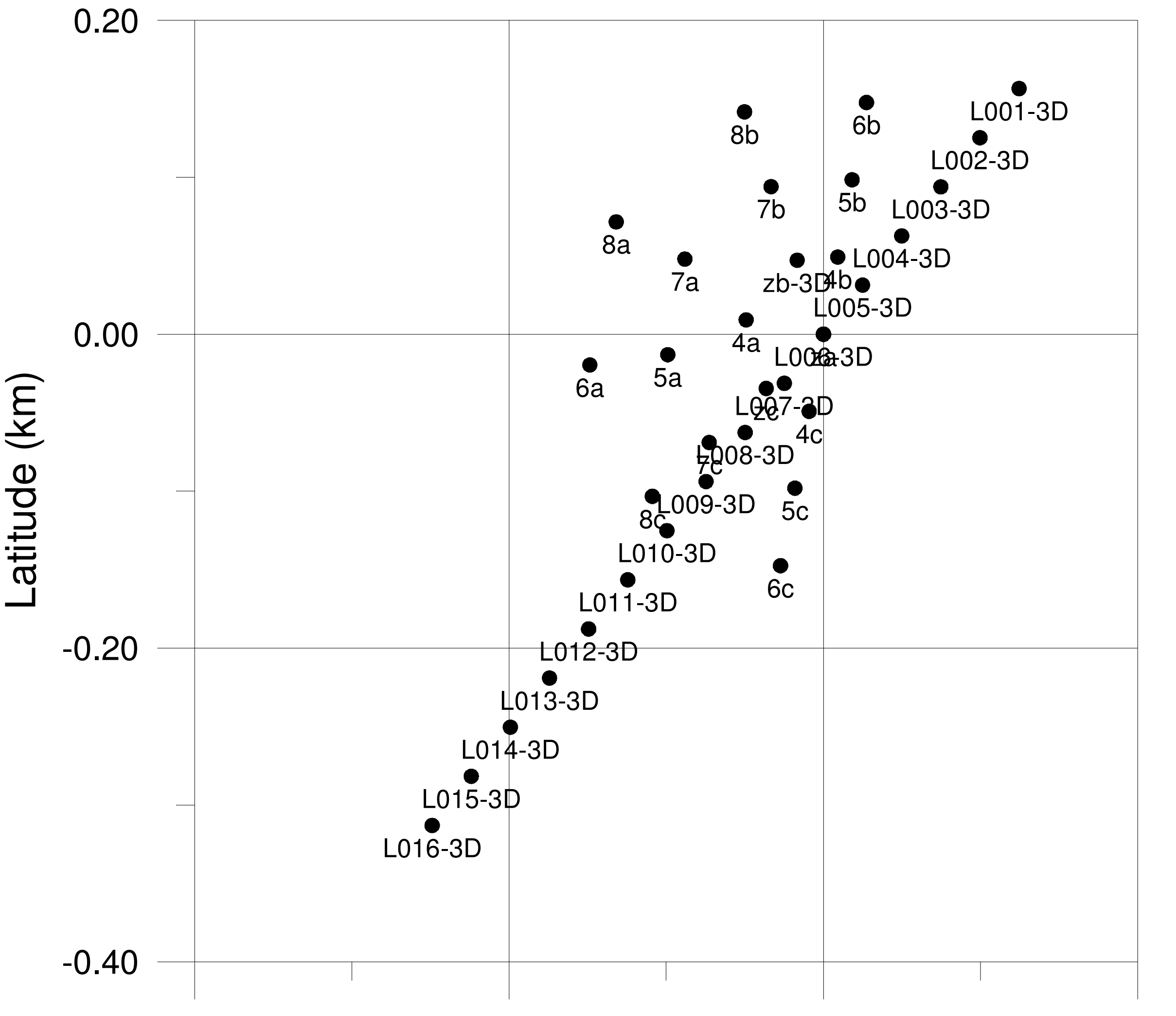
0.20
0.00
-0.20
-0.40
-0.40
-0.20
0.00
0.20
Latitude (km)
Longitude (km)
L001-3D
L002-3D
L003-3D
L004-3D
L005-3D
L006-3D
L007-3D
L008-3D
L009-3D
L010-3D
L011-3D
L012-3D
L013-3D
L014-3D
L015-3D
L016-3D
8b
6b
7b
5b
8a
7a
zb-3D
4b
4a
za
6a
5a
zc
4c
7c
5c
8c
6c

Fig. 3

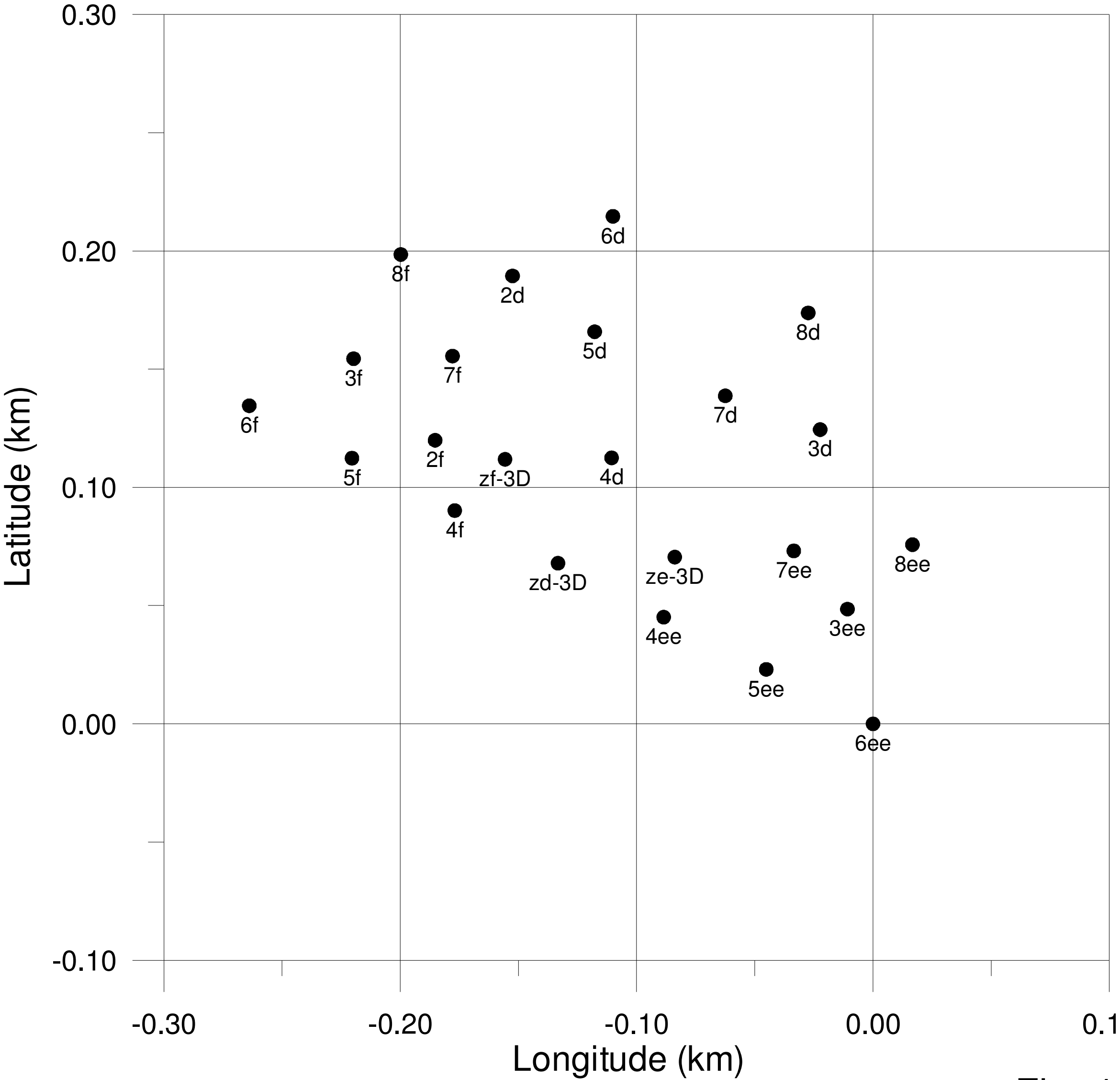
0.30
0.20
0.10
0.00
-0.10
Latitude (km)
-0.30
-0.20
-0.10
0.00
0.10
Longitude (km)
6d
8f
2d
8d
5d
3f
7f
6f
7d
3d
2f
5f
zf-3D
4d
4f
8ee
7ee
zd-3D
ze-3D
3ee
4ee
5ee
6ee

Fig. 4

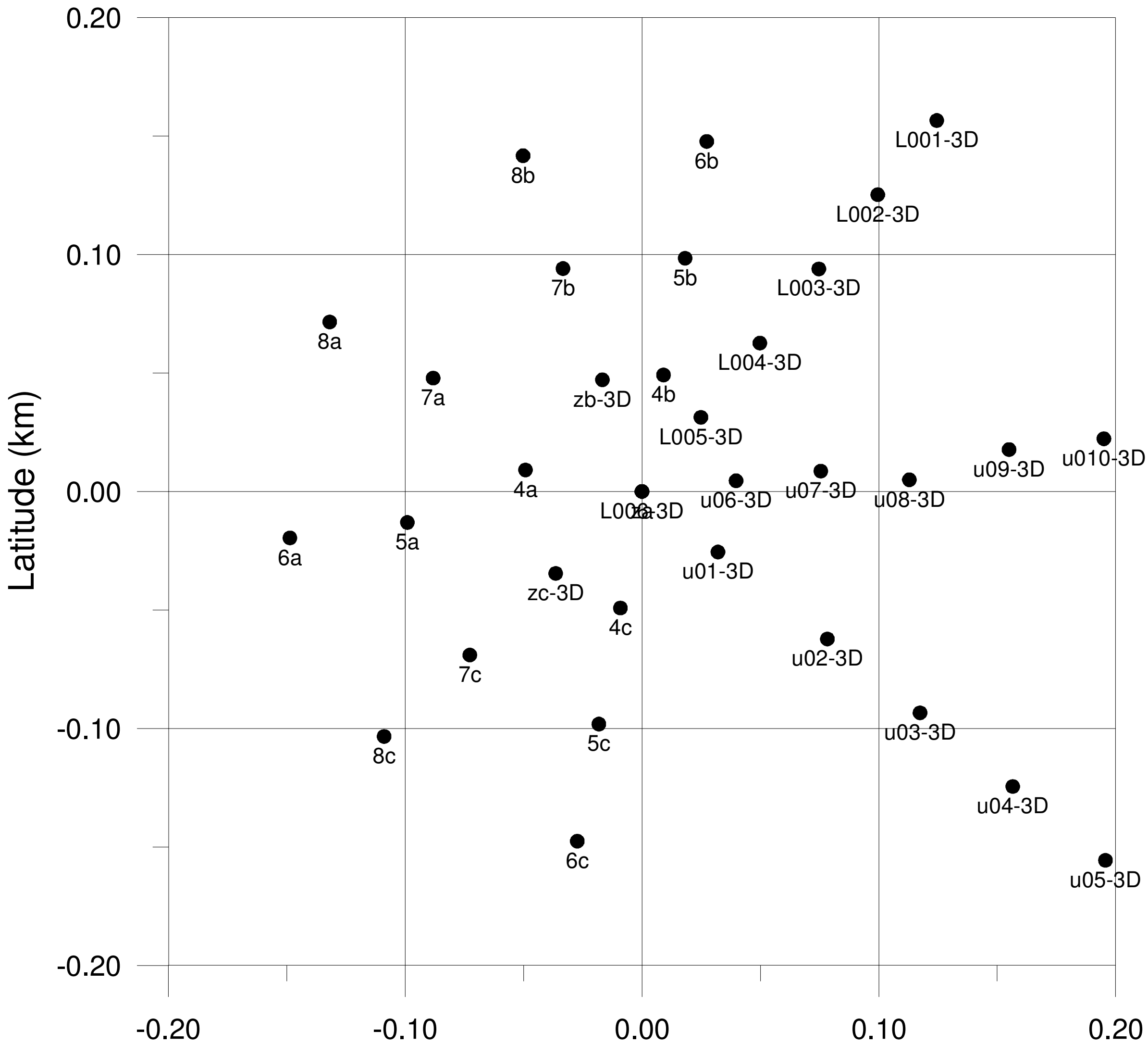
0.20
0.10
0.00
-0.10
-0.20
-0.20
-0.10
0.00
0.10
0.20
Latitude (km)
Longitude (km)
L001-3D
6b
8b
L002-3D
7b
5b
L003-3D
8a
L004-3D
7a
zb-3D
4b
L005-3D
u09-3D
u010-3D
4a
L006-3D
u06-3D
u07-3D
u08-3D
6a
5a
u01-3D
zc-3D
4c
u02-3D
7c
8c
5c
u03-3D
u04-3D
6c
u05-3D

Fig 5

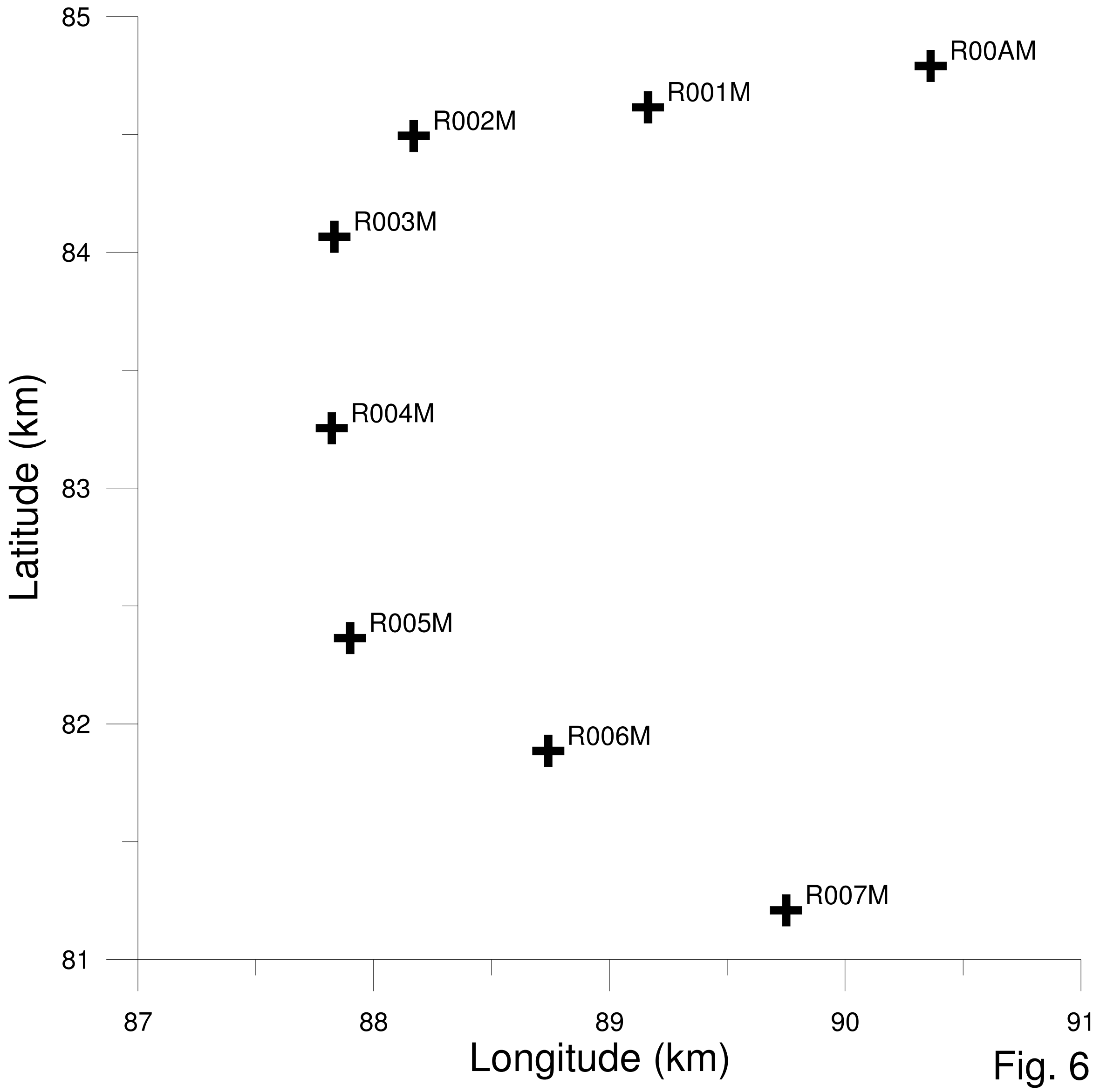

85
84
83
82
81
Latitude (km)
87
88
89
90
91
Longitude (km)
R00AM
R001M
R002M
R003M
R004M
R005M
R006M
R007M


Fig. 6

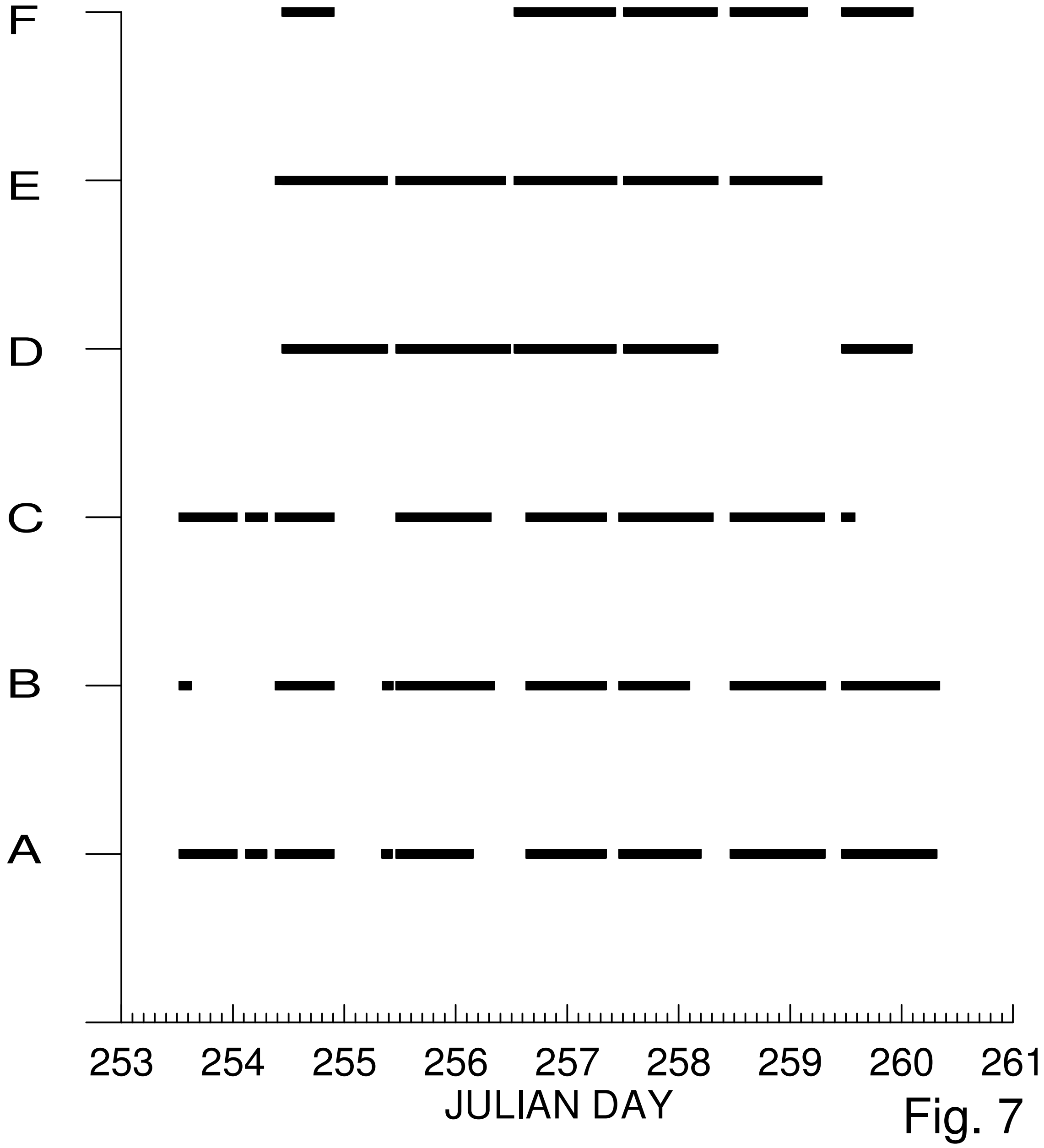


Fig. 7

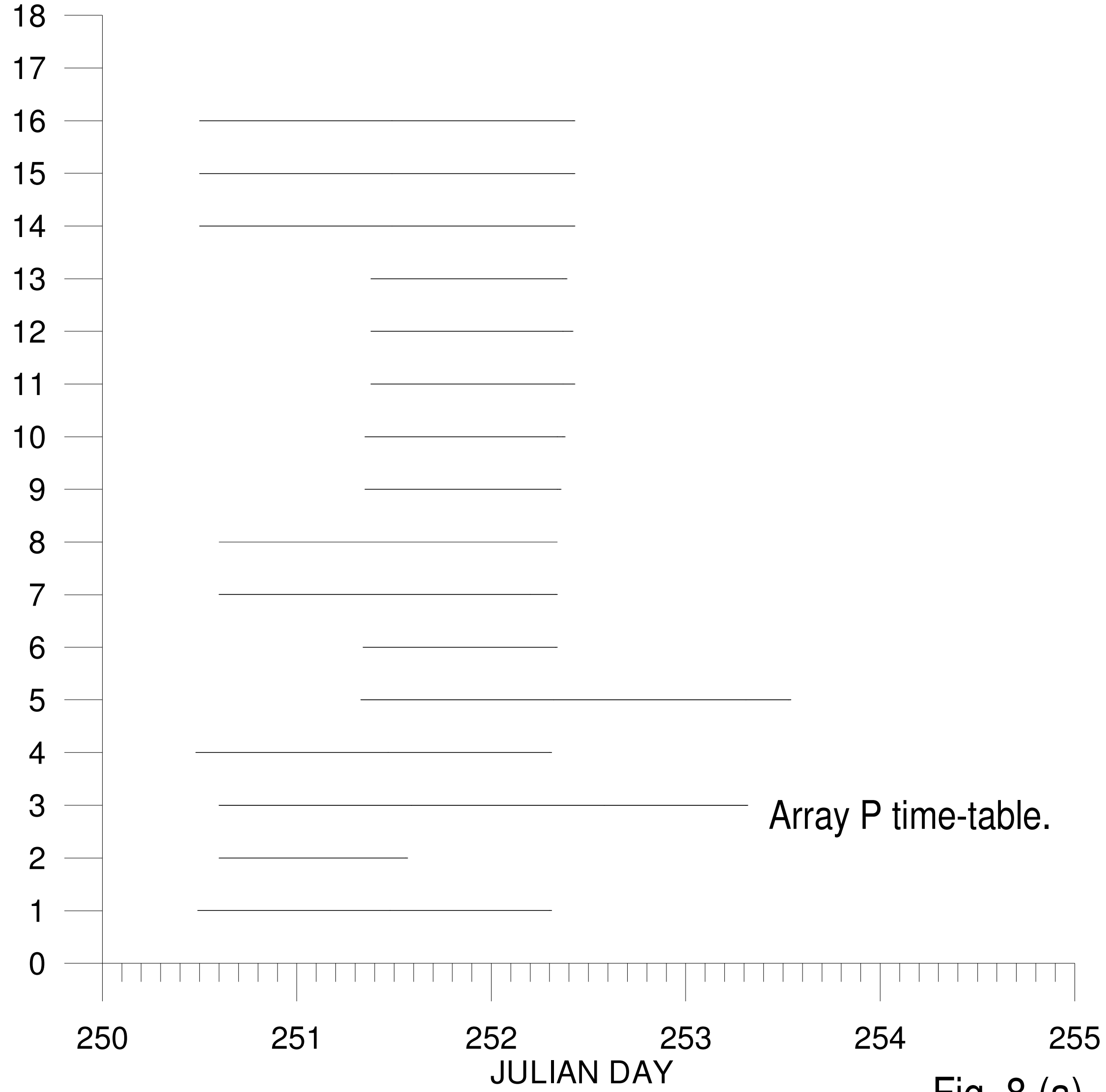

18
17
16
15
14
13
12
11
10
9
8
7
6
5
4
3
2
1
0
250
251
252
253
254
255
JULIAN DAY
Array P time-table.


Fig. 8 (a)

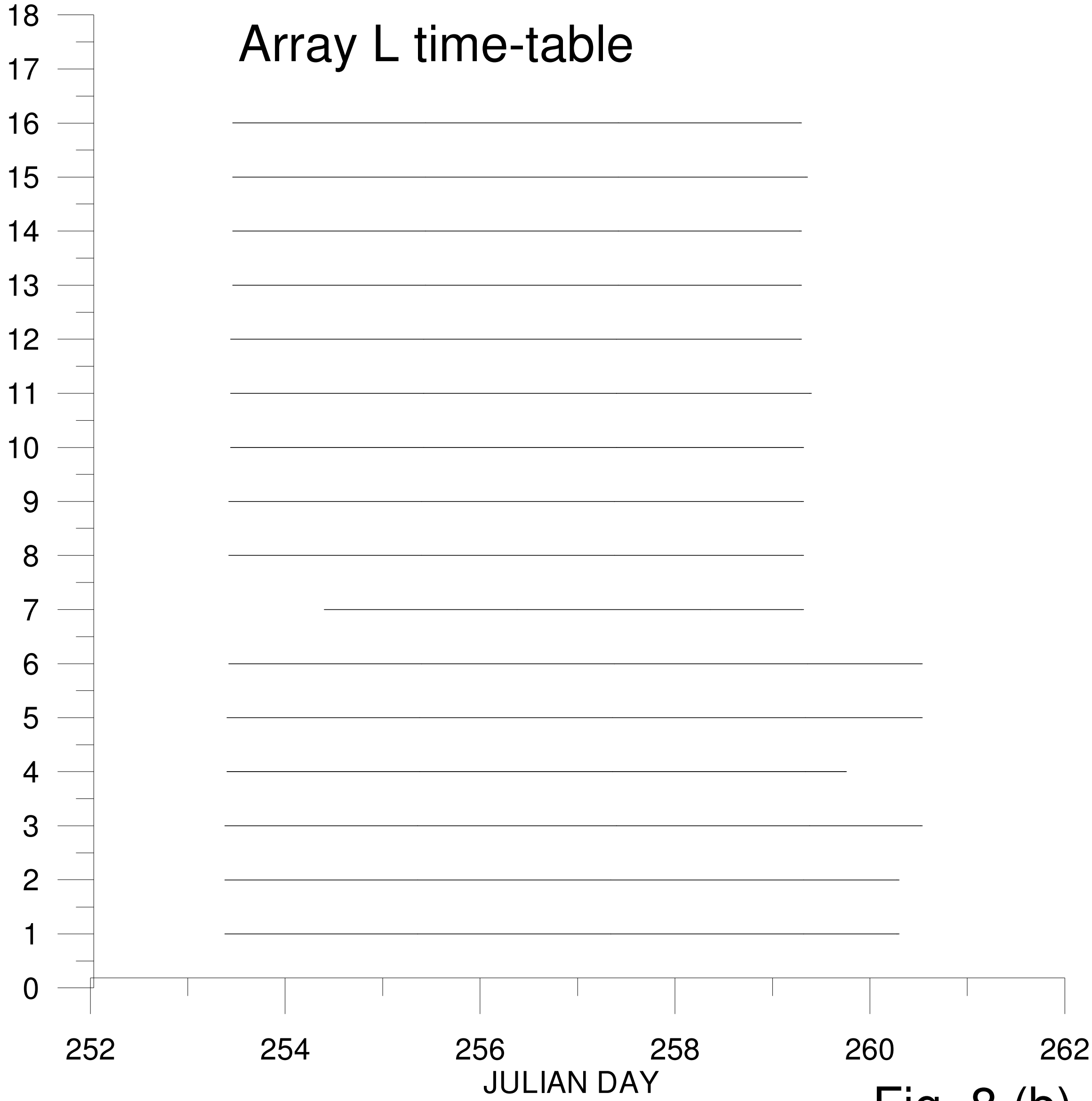
Array L time-table
18
17
16
15
14
13
12
11
10
9
8
7
6
5
4
3
2
1
0
252
254
256
258
260
262
JULIAN DAY

Fig. 8 (b)

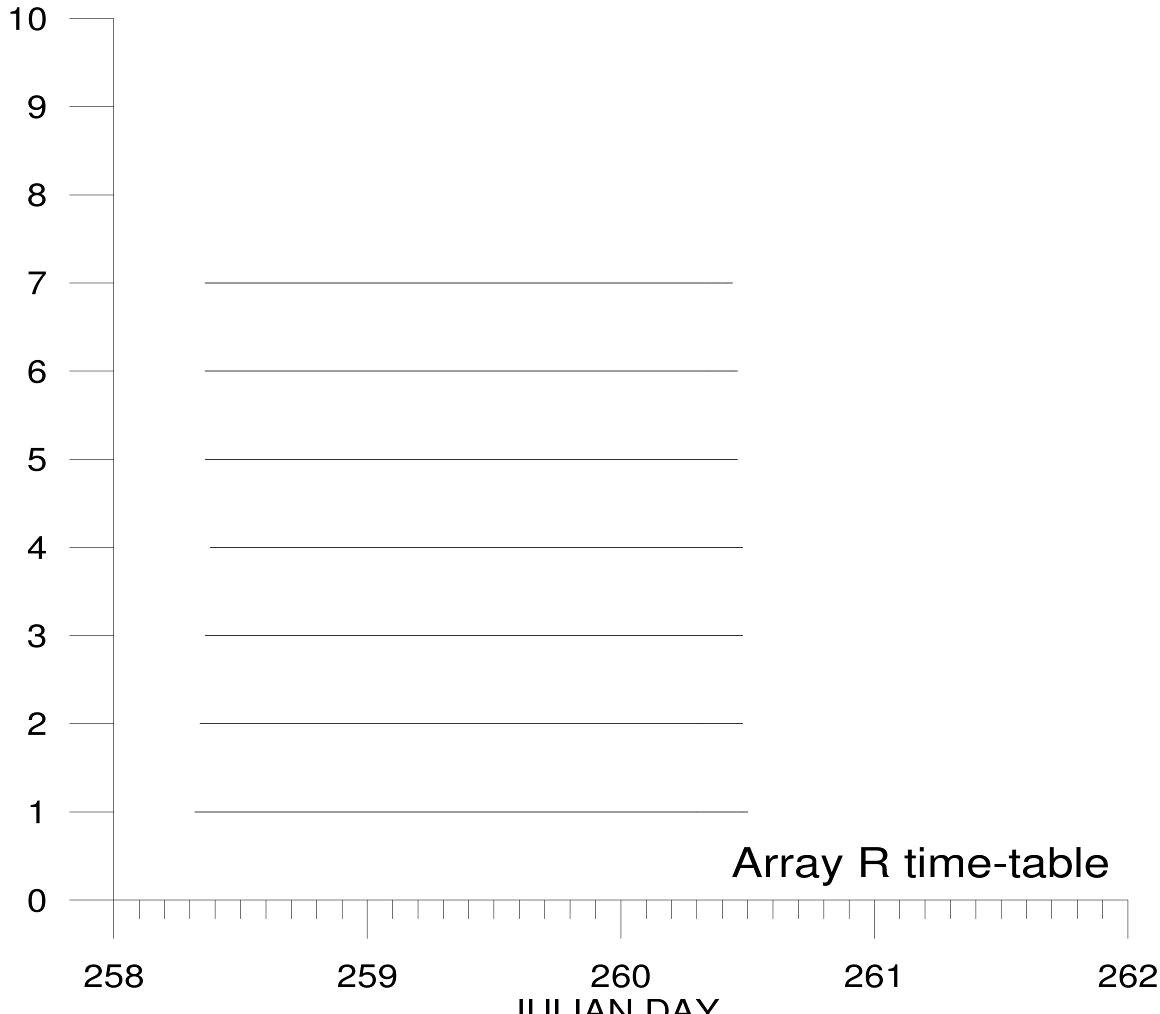
10
9
8
7
6
5
4
3
2
1
0
Array R time-table
258
259
260
261
262
JULIAN DAY
Fig. 8 (c)

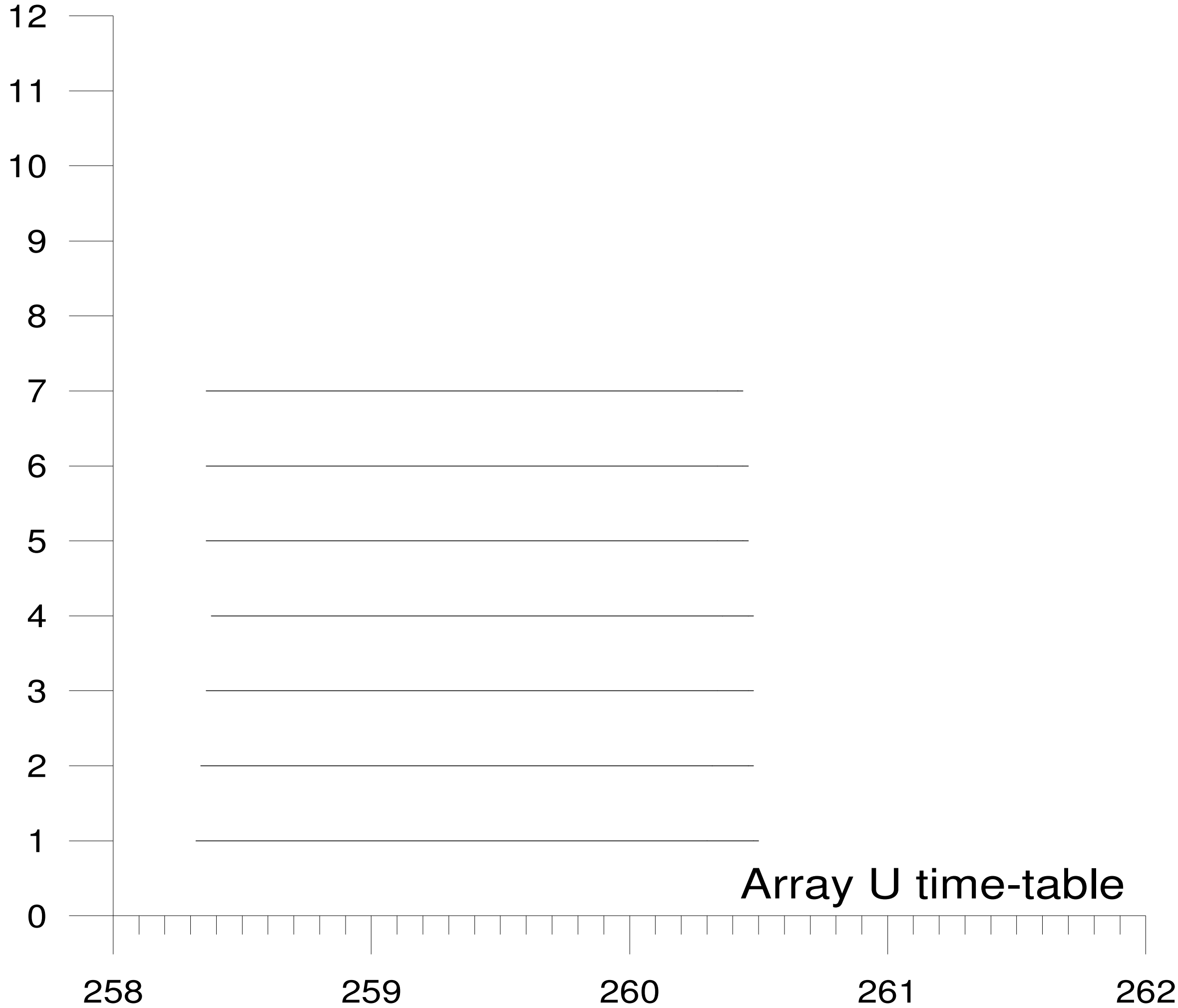

12
11
10
9
8
7
6
5
4
3
2
1
0
Array U time-table
258
259
260
261
262
JULIAN DAY


Fig. 8 (d)

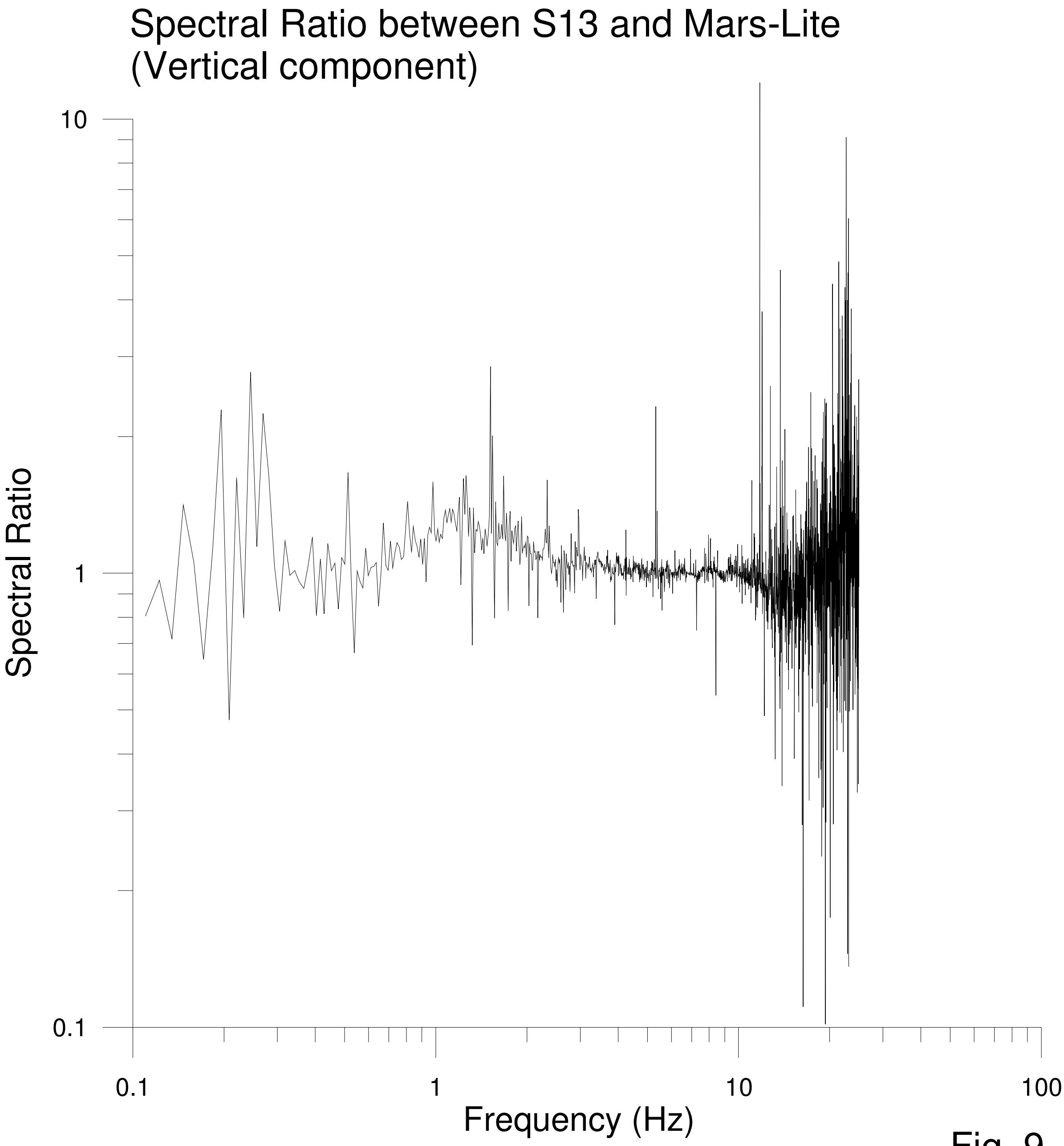

Spectral Ratio between S13 and Mars-Lite
(Vertical component)
10
1
0.1
Spectral Ratio
0.1
1
10
100
Frequency (Hz)


Fig. 9

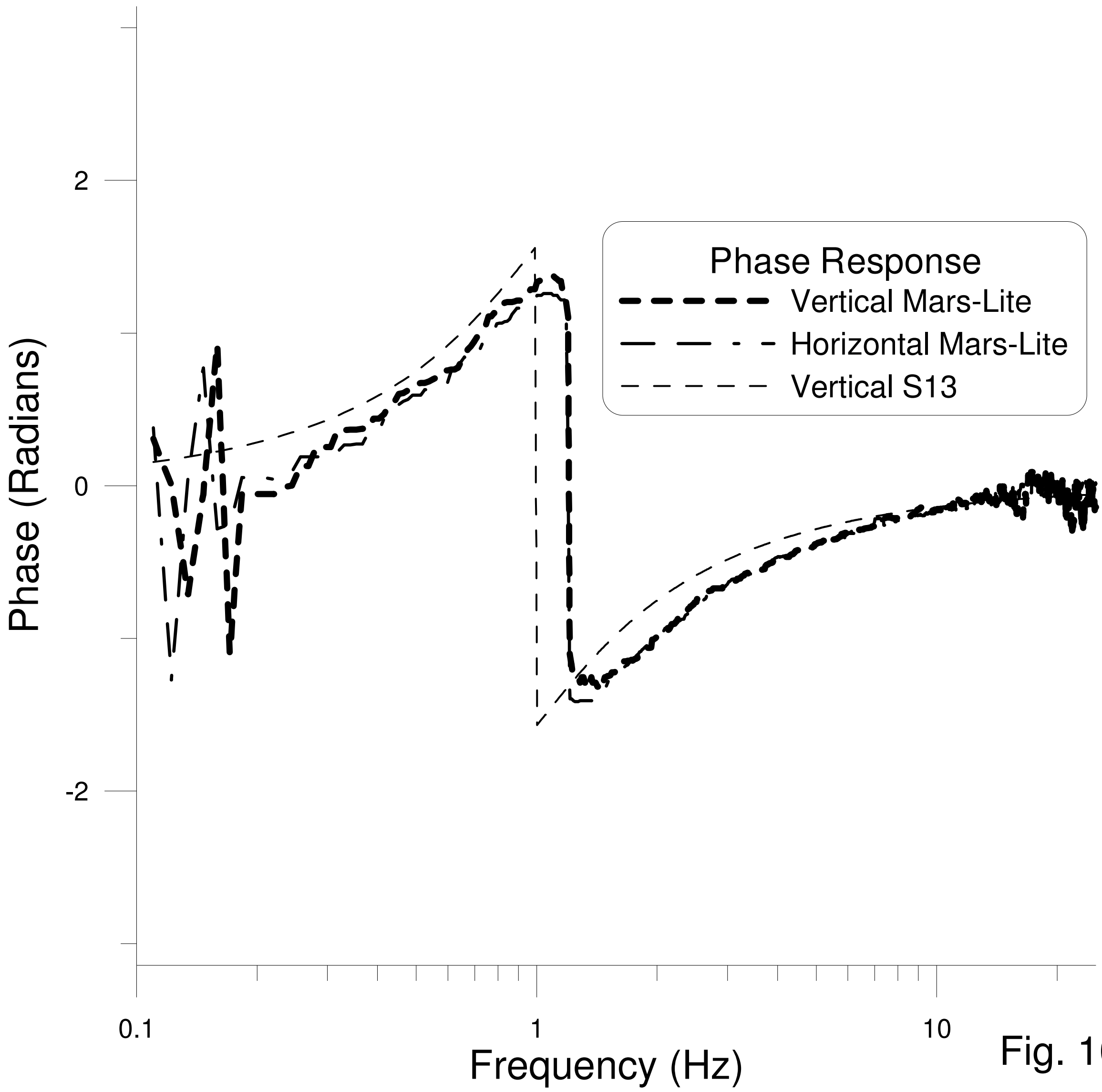

Phase Response
Vertical Mars-Lite
Horizontal Mars-Lite
Vertical S13
Phase (Radians)
2
0
-2
0.1
1
10
Frequency (Hz)


Fig. 10

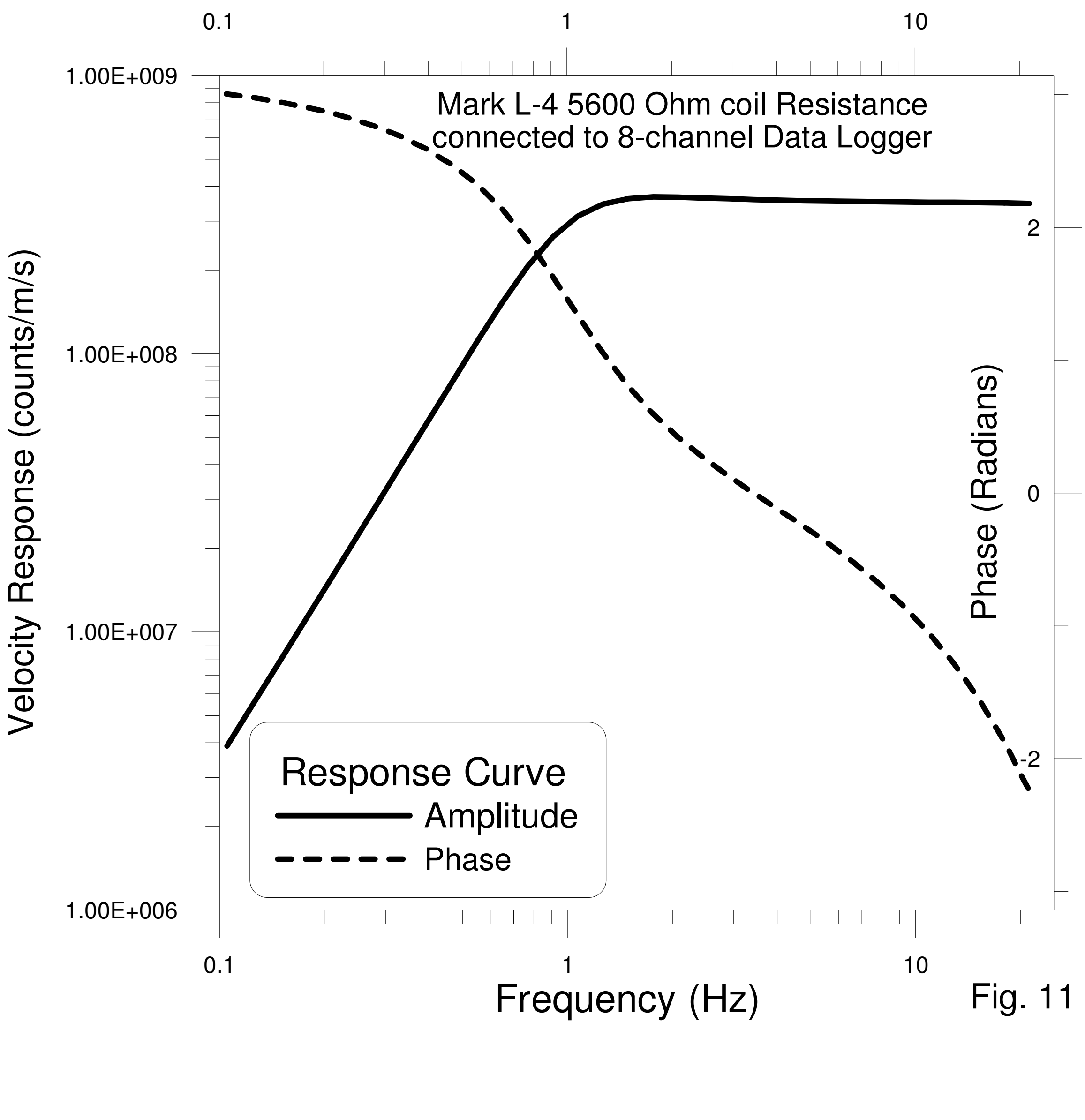

0.1
1
10
1.00E+009
1.00E+008
1.00E+007
1.00E+006
Mark L-4 5600 Ohm coil Resistance
connected to 8-channel Data Logger
2
0
-2
Velocity Response (counts/m/s)
Phase (Radians)
Response Curve
Amplitude
Phase
Frequency (Hz)


Fig. 11

09/13/1999 12:25      Band Pass Filter  0.1 – 10 Hz

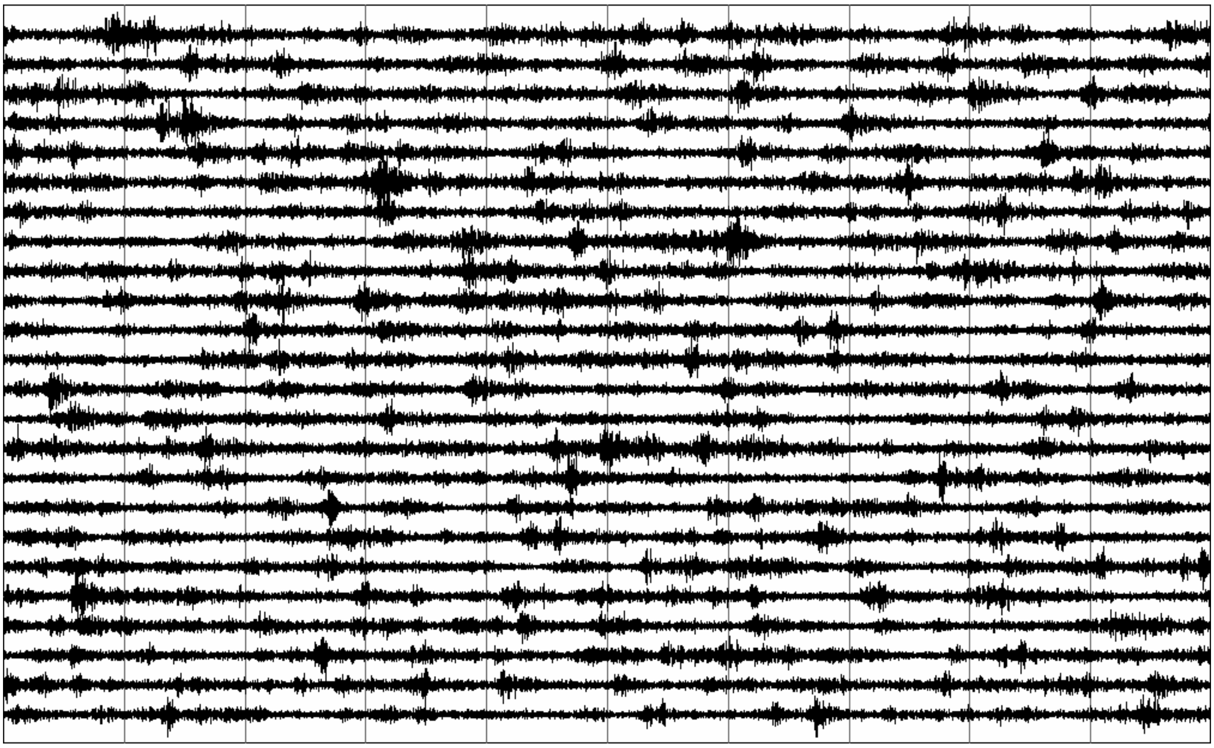

Fig. 12

***ETNA 1999 - ARRAY PIZZI DENERI***

10-09-99 13:49:45.00 GMT VERTICAL COMPONENT

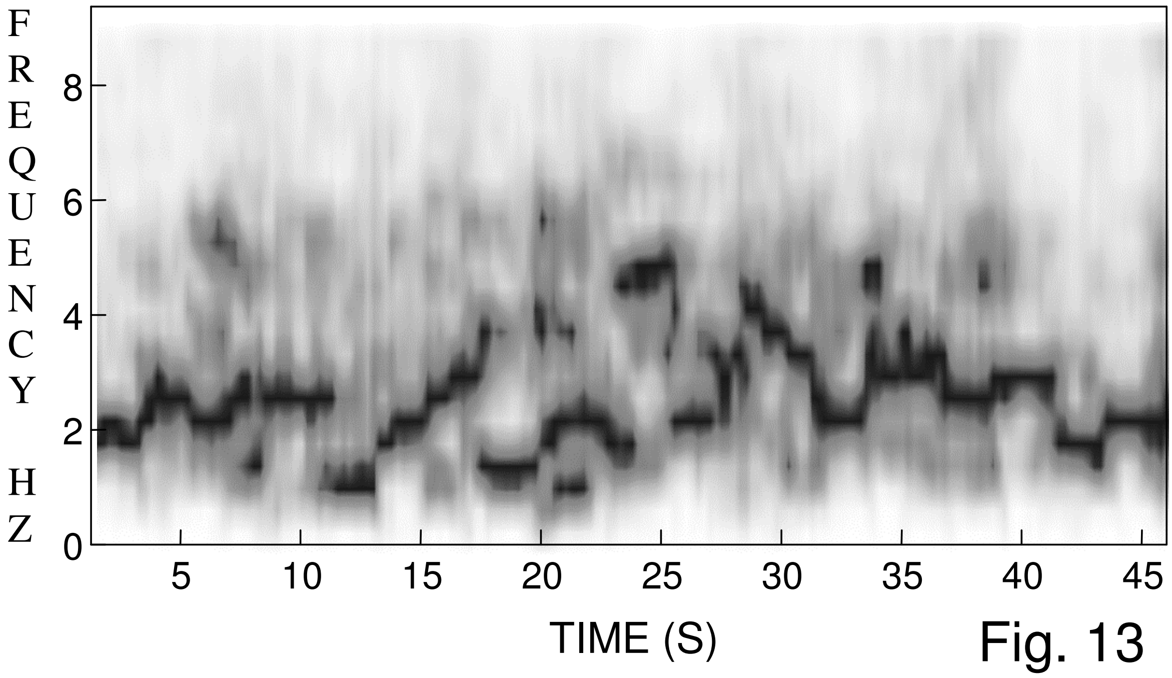


Fig. 13

Fig. 14

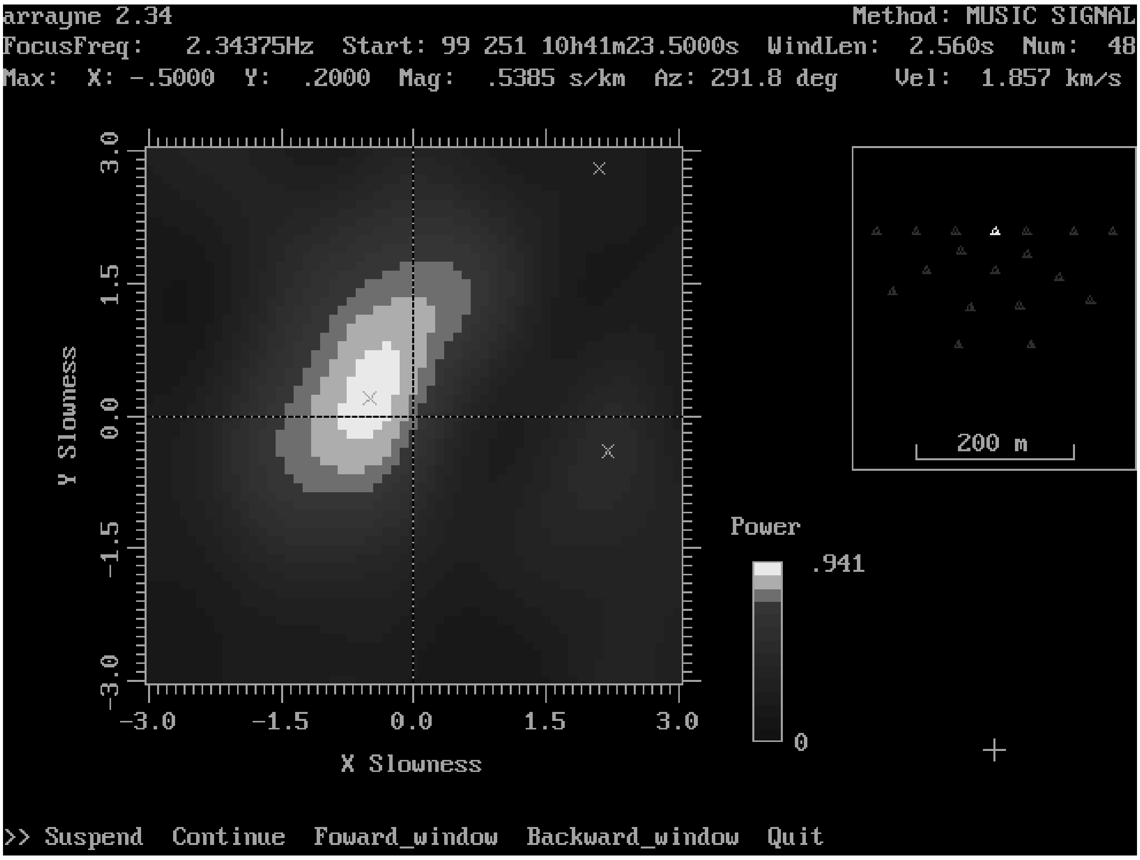

arrayne 2.34
Method: MUSIC SIGNAL
FocusFreq: 2.34375Hz Start: 99 251 10h41m23.5000s WindLen: 2.560s Num: 48
Max: X: -.5000 Y: .2000 Mag: .5385 s/km Az: 291.8 deg Vel: 1.857 km/s
3.0
1.5
0.0
-1.5
-3.0
Y Slowness
-3.0
-1.5
0.0
1.5
3.0
X Slowness
200 m
Power
.941
0
>> Suspend Continue Foward_window Backward_window Quit

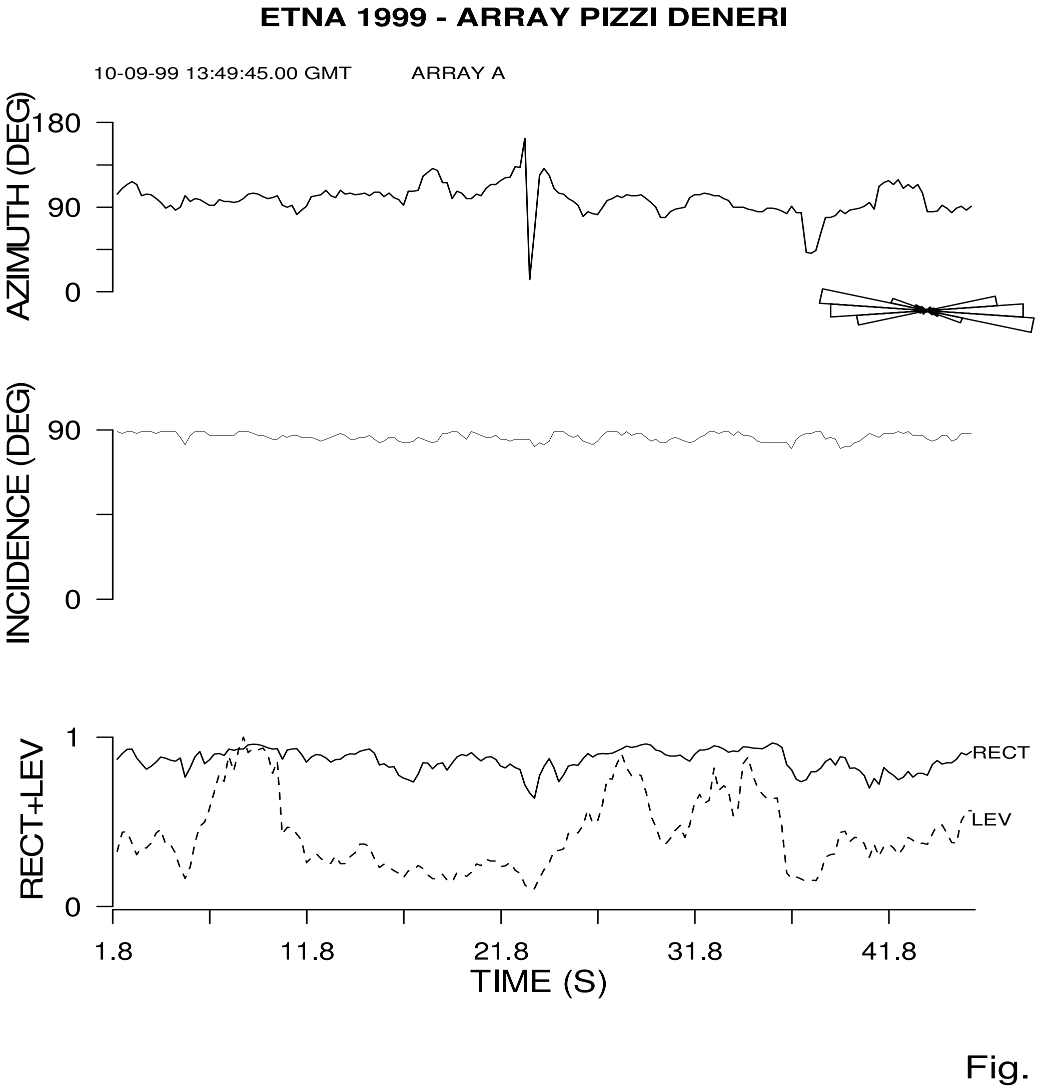

ETNA 1999 - ARRAY PIZZI DENERI
10-09-99 13:49:45.00 GMT
ARRAY A
AZIMUTH (DEG)
180
90
0
INCIDENCE (DEG)
90
0
RECT+LEV
1
0
RECT
LEV
1.8
11.8
21.8
31.8
41.8
TIME (S)


Fig. 15

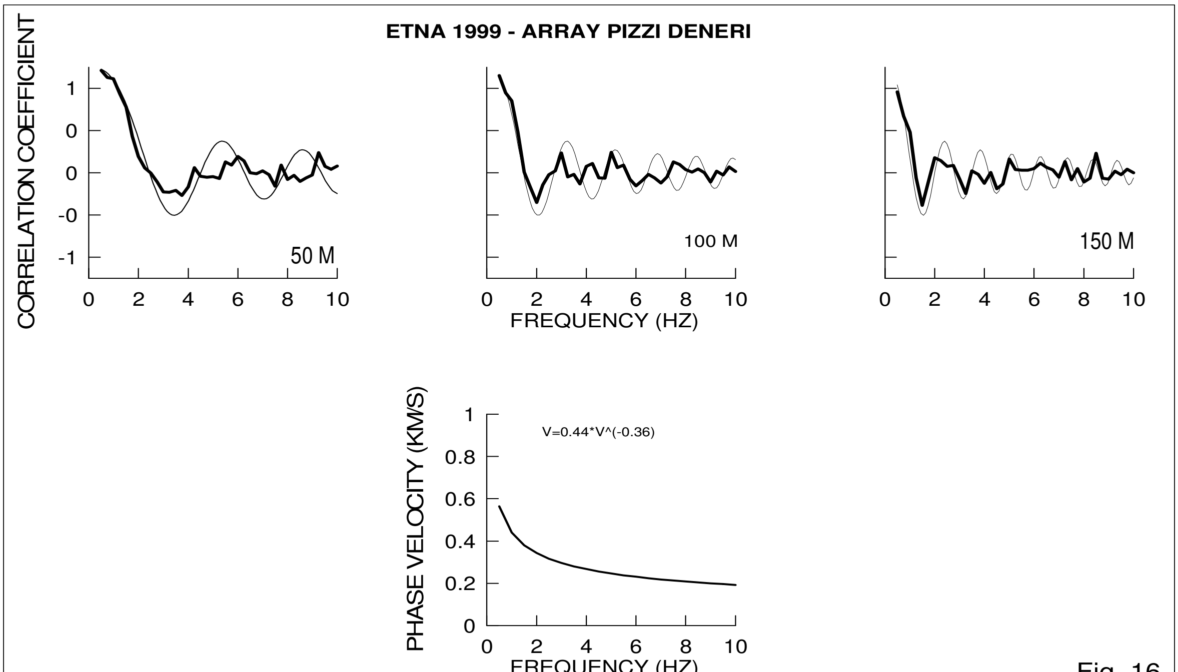

ETNA 1999 - ARRAY PIZZI DENERI
CORRELATION COEFFICIENT
1
0
0
-0
-1
50 M
100 M
150 M
0 2 4 6 8 10
FREQUENCY (HZ)
PHASE VELOCITY (KM/S)
V=0.44*V^(-0.36)
1
0.8
0.6
0.4
0.2
0


Fig. 16